

CS754 ASSIGNMENT 1

Hitesh Kumar Punna, Sudhansh Peddabomma

190050093, 190050118

Question 1.

- (1) In compressed sensing we want our signals to be sparse for better reconstruction. This statement is not against the premise of compressed sensing. Think of it this way, we don't know the sparsity of θ . Hence, we take a ballpark estimate of s and apply theorem 3. Now suppose we choose $s = 10$. If θ is 100-sparse, then the no of non-zero values in θ can range from 0 – 100. If θ is more sparse, i.e there are less no of non-zero values, then the upper bound on the RHS is lesser (for a chosen s). For example, if θ has 70 non-zero values, then the upper bound is non-zero. But, if θ has only 5 non-zero values then the upper bound is 0 (ignoring the error term). Therefore, if the signal is more sparse then we have a lower reconstruction error. This is not against the premise of compressed sensing. This may be easier to think about by considering the fact that signals with s non-zero values are also $s + k$ sparse for $k \in \mathbb{N}$.

Now coming to the point that the upper bound decreases as s increases. This is true if s is less than the no of non-zero values in θ . The upper bound is already 0 (ignoring the error term in RHS) if the signal is s' -sparse where $s' < s$. If θ is less sparse, then we obviously need larger s to get a better bound. This requires the measurement matrix Φ to have $\delta_{2s} < 0.41$ for a larger s . This indirectly increases m (the no of rows in Φ) because $m \geq c_\delta \log(n/\delta)$. This is not desirable in the compressed sensing domain.

In conclusion, if a signal is more sparse, it reaches a better upper-bound faster than a signal which is less sparse, as s increases.

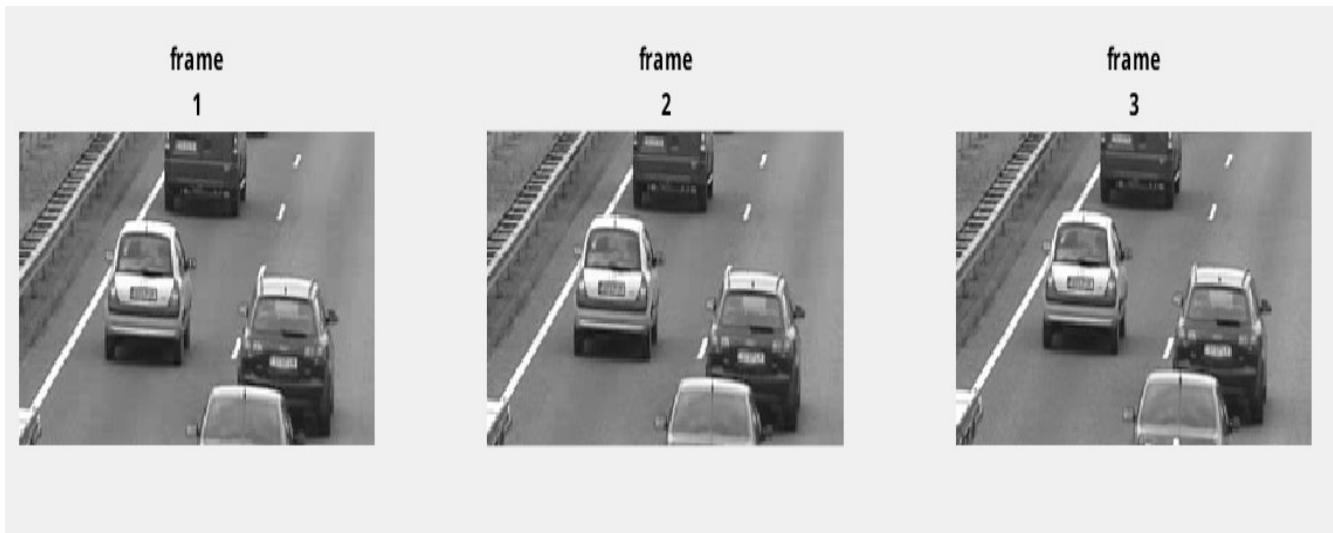
- (2) As we know $m \geq c_{\delta_s} \log(n/s)$, where $c_{\delta_s} = \frac{0.18}{\log((1+\delta_s/(1-\delta_s))+1)}$ ¹, we can say that m has to increase as δ_s increases. Also, ϕ needs to obey RIP with δ_{2s} close to 0. We know that the numebr of rows of ϕ , $m \geq 2s$ for this to happen. That is, $m < 2s$ then any $2s$ columns of ϕ will not be linearly independent and an S -sparse vector will lie in the null space of ϕ . Hence, as the upper bound depends on δ_{2s} through C_0 and C_1 , and δ_{2s} depends on m , the error bound depends on m indirectly.
- (3) Theorem 3 is more useful than Theorem 3A. This is because, Theorem 3 allows us to choose Measurement matrices that have a higher δ_{2s} in comparison to Theorem 3A. To construct Measurement matrices with low δ_s values we start by choosing a random matrix and try to minimize the mutual coherence of matrix A . We know $\delta_s < \mu(S-1)$, from this we can say that lower the value of Mutual Coherence of matrix A the lower will be the δ_{2s} . So choosing δ_{2s} with higher upper bound will result in easier construction of Measurement matrix. Now, the upper bound for δ_s in theorem 3 is 0.41, and 0.3 in theorem 3A so from our previous analogy we can say that Theorem 3 is more useful than Theorem 3A.
- (4) Firstly, substituting $\varepsilon = 0$ would be wrong, because we choose $\varepsilon \geq |\eta|^2$ for solving the BP problem, and taking $\varepsilon = 0$ would violate this condition when the noise is non-zero. Hence, we can't use Theorem 3 to determine the bound of the error.

Secondly, the θ we get by solving BP problem with $\varepsilon = 0$ satisfies $y = \Phi\Psi\theta + \eta$ and is noisy. Hence, we don't get a proper reconstruction. Further, the θ obtained this way may not be a better solution than the θ obtained by solving BP with $|y - \Phi\Psi\theta| \leq \varepsilon \neq 0$. That is, we allow our algorithm to explore more sparse vectors by allowing $\varepsilon \geq |\eta|^2$ which may yield us the correct solution.

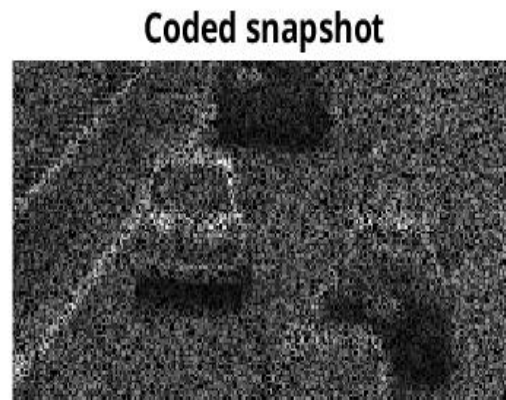
¹cited from [Restricted Isometry Property](#)

Question 2.

(a) The 3 extracted frames are



(b) The coded aperture image for $T = 3$



(c) The masking was implemented in the following way:

$$E_u = C_1.F_1 + C_2.F_2 + C_3.F_3 + \dots + C_T.F_T$$

To write the above equation in $Ax = b$ form, we proceed in the following way.

Note that, vector (C) gives a $MN \times 1$ matrix of all columns concatenated as a column vector where C is a $M \times N$ matrix

and, $D = \text{diag}(Y)$ gives a diagonal matrix with diagonal elements being the elements of vector Y . D is of the form,

$$D = I \cdot Y = \begin{bmatrix} y_1 & 0 & \cdot & \cdot & \cdot & 0 \\ 0 & y_2 & 0 & \cdot & \cdot & 0 \\ \cdot & & & & & \\ \cdot & & & & & \\ 0 & \cdot & \cdot & \cdot & 0 & y_n \end{bmatrix}, \text{ where } Y = [y_1 \quad \cdot \quad \cdot \quad \cdot \quad y_n]^T$$

Construct the matrices, C''_i where $i \in [T]$ and C' as follows

$$C''_i = \text{diag}(\text{vector}(C_i)) \text{ and } C'_i = \text{vector}(C_i) \text{ for each } i \in \{1, 2, \dots, T\}$$

Construct A as,

$$A = [C''_1 \quad C''_2 \quad \cdot \quad \cdot \quad C''_T]$$

Dimension of A is $n \times nT$ T = number of frames; $n = H \times W$;

Similarly, construct F'_i as

$$F'_i = \text{vector}(F_i) \text{ for each } i \in \{1, 2, \dots, T\}$$

Then,

$$x = [F'_1 \quad F'_2 \quad \cdot \quad \cdot \quad F'_T]^T \text{ and } b = \text{vector}(E)$$

Now, we claim that $Ax = b$ represents the first equation

Let $E_{i,j}$ be the element in i th row and j th column in matrix E . From the definition, $E_{i,j} = \sum_{t=1}^T (C_t)_{i,j} (F_t)_{i,j}$

Now from the equation $Ax = b$,

$$b_k = \sum_{i=1}^{nT} (A_{k,i}) (x_{i,1}) \text{ as } A = [C''_1 | C''_2 | \dots | C''_T] \text{ and } C''_i = \text{diag}(\text{vector}(C_i))$$

From this we can say $A_{k,i} = 0$ if $i \neq jT + k$ where $j \in \{0, 1, 2, \dots, n-1\}$

Therefore, $b_k = \sum_{j=1}^n (A_{k,jT+k}) (x_{jT+k,1})$

Now, $A_{k,jT+k} = (C''_j)_{k,k} = (C'_j)_{k,1}$ and $x_{jT+k,1} = (F'_j)_{k,1}$ [$(F'_i)_{x,1}$ represents x th element of i th frame vector]

$b_k = \sum_{j=1}^n (C'_j)_{k,1} (F'_j)_{k,1}$ as we know $E_{x,y} = b_{(x*W+y)}$, $(C_j)_{x,y} = (C'_j)_{(x*W+y),1}$, $(F_j)_{x,y} = (F'_j)_{(x*W+y),1}$ where E, F, C are $W \times H$ matrices [$(F_i)_{x,y}$ represents the pixel (x, y) in i th frame]

$$b_{(x*W+y)} = \sum_{j=1}^n (C'_j)_{(x*W+y),1} (F'_j)_{(x*W+y),1} = \sum_{j=1}^n (C_j)_{x,y} (F_j)_{x,y}$$

Therefore $E_{x,y} = \sum_{j=1}^n (C_j)_{x,y} (F_j)_{x,y}$

Hence, our substitution $Ax = b$ represents the coded snapshot equation.

(d) Similar to the previous constructions, we can construct an equation of the form $Mx' = y$ for each patch.

Consider A, b and x as defined in the (c) part. Now, for a patch $p = (i, j)$ which represents the pixels in the $8 \times 8 \times T$ sub-matrix with p as top-left corner in each frame. Let the pixels in patch p correspond to the set of indices l in x . We construct M from the patches of binary mask which correspond to patch p in the same way as described in (c) part. That is, $y = Mx'$ where,

$$M = \begin{bmatrix} C_1(i, j) & 0 & \cdot & C_2(i, j) & 0 & \cdot & C_3(i, j) & 0 & \cdot \\ 0 & C_1(i+1, j) & \cdot & 0 & C_2(i+1, j) & \cdot & 0 & C_3(i+1, j) & \cdot \\ \cdot & & & & & & & & \\ 0 & 0 & C_1(i+7, j+7) & \cdot & \cdot & C_2(i+7, j+7) & \cdot & 0 & C_3(i+7, j+7) \end{bmatrix}$$

Here, $C_i(x, y)$ represents the value at the pixel (x, y) in the randomly generated 2D coded aperture used for the i th frame.

$$x' = \begin{bmatrix} F_1(i, j) \\ F_1(i+1, j) \\ \vdots \\ F_1(i+7, j) \\ F_1(i, j+1) \\ \vdots \\ F_1(i+7, j+1) \\ \vdots \\ F_1(i+7, j+7) \\ F_2(i, j) \\ \vdots \\ F_2(i, j+1) \\ \vdots \\ F_2(i+7, j+7) \\ \vdots \\ F_T(i, j) \\ \vdots \\ F_T(i+7, j+7) \end{bmatrix}$$

The OMP algorithm is present in Q2.m as the function OMP(y, A, psi). Note that, we can't use OMP directly on x as x is not sparse. Hence, we construct a 2D DCT basis matrix to get θ which is sparse.

The 2D DCT matrix is constructed from *Kronecker product* of individual 8x8 1D DCT matrices. Let us call the 2D DCT matrix D . And then, we use a block matrix of T D matrices as our Ψ . That is

$$\Psi = \begin{pmatrix} D & & & \\ & D & & \\ & & \ddots & \\ & & & D \\ & & & & D \end{pmatrix}$$

This calculates the DCT coefficients of each frame individually. Hence, we get 2D DCT coefficients of each frame separately.

Now, the ε for the OMP algorithm is chosen as follows. We know that noise in $y = A\Psi\theta$ is Gaussian with variance 2. That is, $\eta_i \sim N(0, 4)$ for all $i \in [m]$. Then, the squared magnitude of the vector η is a chi-squared random variable. We know that the magnitude of η will lie within 3 standard deviations from the mean with a very high probability. $P(x^2 < 9\sigma^2) = 0.997$ where $x \sim N(0, \sigma^2)$

Therefore, $\varepsilon = 9m\sigma^2$

Now, $m = 8 * 8$ for a patch and $\sigma^2 = 4$. Hence, $\varepsilon = 4 * 64 * 9 = 2304$

The probability that $|\eta|^2$ is less than ε is $P(|\eta|^2 < \varepsilon) = (0.997)^{64} \approx 0.825$.

(e) The reconstructed images are in Q2_results and have been labelled accordingly. The code is present in q2.m.

The MSE is calculated as $\|F' - F\|_2^2 / \|F\|_2^2$, where F' is the reconstructed image and F is the original image. The MSE value for 3 the frames is $[1.14, 1.09, 1.15] \times 10^{-2}$ and 1.12×10^{-2} for the whole data.

(f) The MSE values of 5 frames are $[2.00, 2.07, 2.01, 1.94, 1.91] \times 10^{-2}$ and 1.989×10^{-2} for the whole data.

The MSE values of 7 frames are $[3.12, 3.48, 3.37, 3.47, 3.39, 3.26, 3.34] \times 10^{-2}$ and 3.35×10^{-2} for the whole data.

(h) The MSE values of the flame video for

3 frames $[6.97, 7.05, 7.47] \times 10^{-4}$ and 7.15×10^{-4} for the whole data

5 frames $[1.13, 1.08, 1.18, 1.23, 1.33] \times 10^{-3}$ and 1.19×10^{-3} for the whole data

7 frames $[4.72, 3.89, 5.20, 3.75, 3.71, 3.89, 3.81] \times 10^{-3}$ and 4.142×10^{-3} for the whole data

Question 3.

Coherence between two matrices Φ and Ψ is defined as

$$\mu(\Phi, \Psi) = \sqrt{n} \max_{i,j \in \{0,1,\dots,n-1\}} |\Phi^i \Psi_j|$$

In conclusion, if a signal is more sparse, it reaches a better upper-bound faster than a signal which is less sparse, as s increases.

Claim. The lower bound of coherence is 1.

Consider a row vector g of the form $g = \sum_{k=1}^n \alpha_k \Psi_k$, where Ψ_i is the i th column of the orthonormal basis Ψ . Now, coherence

$$\mu(g, \Psi) = \frac{\sqrt{n} \max_{i \in [n]} |(\sum_{k=1}^n \alpha_k \Psi_k) \cdot \Psi_i|}{|g|}$$

Further, for all i, j , $\Psi_i \cdot \Psi_j = 0$ if $i \neq j$ and 1 otherwise. Hence,

$$\mu(g, \Psi) = \frac{\sqrt{n} \max_{i \in [n]} |\alpha_i|}{\sqrt{\sum_{i=1}^n \alpha_i^2}}$$

Now suppose, coherence is lesser than 1 for the sake of contradiction.

$$\mu(g, \Psi) < 1 \implies \max_{i \in [n]} |\alpha_i| < \frac{\sqrt{\sum_{i=1}^n \alpha_i^2}}{\sqrt{n}} \implies \forall i \in [n] \alpha_i < \frac{\sqrt{\sum_{i=1}^n \alpha_i^2}}{\sqrt{n}} \implies \sum_{i=1}^n \alpha_i^2 < \frac{\sum_{i=1}^n \alpha_i^2}{n} \implies n < 1$$

This is a contradiction. Therefore, the claim holds.

Claim. The upper bound of coherence is \sqrt{n} .

Consider a row vector g of the form $g = \sum_{k=1}^n \alpha_k \Psi_k$, where Ψ_i is the i th column of the orthonormal basis Ψ . Now, coherence

$$\mu(g, \Psi) = \frac{\sqrt{n} \max_{i \in [n]} |(\sum_{k=1}^n \alpha_k \Psi_k) \cdot \Psi_i|}{|g|}$$

Further, for all i, j , $\Psi_i \cdot \Psi_j = 0$ if $i \neq j$ and 1 otherwise. Hence,

$$\mu(g, \Psi) = \frac{\sqrt{n} \max_{i \in [n]} |\alpha_i|}{\sqrt{\sum_{i=1}^n \alpha_i^2}}$$

Now suppose, coherence is greater than \sqrt{n} for the sake of contradiction.

$$\mu(g, \Psi) > \sqrt{n} \implies \max_{i \in [n]} |\alpha_i| > \sqrt{\sum_{i=1}^n \alpha_i^2} \implies \sum_{i \in [n] \setminus \{\arg\max_i \alpha_i\}} \alpha_i^2 < 0$$

This is a contradiction. Therefore, the claim holds.

Now, for any normalised measurement matrix Φ , coherence is

$$\mu(\Phi, \Psi) = \sqrt{n} \max_{i,j \in \{0,1,\dots,n-1\}} |\Phi^i \Psi_j| \equiv \max_{i \in \{0,1,\dots,n-1\}} \mu(\Phi_i, \Psi)$$

Hence, the value of coherence lies between 1 and \sqrt{n} .

Question 4.

- (a) No, we cannot determine x with $m = 1$. Let the i th element of x be non-zero. Then consider a row-vector Φ of length n . Then, $y = \Phi x = \Phi_i x_i$. Here, we can find the value of the non-zero element but we cannot determine the *index* of the non-zero element in x .

If we know the index of the non-zero element in x , then we can easily find x from $y = \Phi_i x_i$. That is,

$$x = [0 \quad 0 \quad \dots \quad \frac{y}{\Phi_i} \quad \dots \quad 0]^T$$

Note: We can always find a solution when the index is given except for the cases in which $\Phi_i = 0$ as Φ is randomly generated.

- (b) Yes, we can find the non-zero value with $m = 2$ in most of the cases. This can be done in the following way. Consider Φ of the form,

$$\Phi = \begin{bmatrix} \Phi_{11} & \Phi_{12} & \dots & \Phi_{1i} & \dots & \Phi_{1n} \\ \Phi_{21} & \Phi_{22} & \dots & \Phi_{2i} & \dots & \Phi_{2,n} \end{bmatrix}$$

Let $y = [y_1, y_2]^T$ be the measured data, then let x_i be the non-zero element of vector x (i is the index at which it's non-zero).

Hence,

$$y_1 = \Phi_{1i} x_i \text{ and } y_2 = \Phi_{2i} x_i \implies \Phi_{1i} / \Phi_{2i} = y_1 / y_2$$

If we choose the matrix Φ such that for each $i \in [n]$, Φ_{1i} / Φ_{2i} is unique, then we can uniquely determine x . Also, ϕ must be incoherent with the canonical basis, else the data might be lost in Φx . Incoherence should ensure, Φ_{2i} and Φ_{1i} are non-zero for unique determination.

- (c) We cannot uniquely estimate the x matrix.

We use the fact that any four 3D-vectors are **not linearly independent** to prove the above claim.

We can find x_1, x_2 such that $\phi(x_1 - x_2) = 0$. Here x_1, x_2 are 2-sparse elements each hence $x_1 - x_2$ will be a 4-sparse vector.

$$\phi(x_1 - x_2) = x_{i_1} \phi_{i_1} + x_{i_2} \phi_{i_2} + x_{i_3} \phi_{i_3} + x_{i_4} \phi_{i_4}$$

Because the above equation represents the linear combination of 4 3D vectors, there exist some $x_1 - x_2$ such that the above expression equates to 0. If we can't find any x_1 and x_2 which satisfy an equation of the above form, then 4 columns of Φ are linearly independent. But this is a contradiction.

From this, we can say that we can't reconstruct x uniquely from $y = \phi x$. Note that, $m \geq 2S$ for unique reconstruction of an S -sparse signal. Here, m has to be ≥ 4 , which is not true. Hence, unique reconstruction is not possible.

- (d) Yes, we can uniquely estimate the x matrix, if ϕ satisfies the property that any 4 columns in ϕ are linearly independent. We prove it as follows

Note. If number of rows in each ϕ_i equal to 4, then the size of any subset of linearly independent columns does not exceed 4. (i.e more than 4 column vectors won't be linearly independent)

Let's say there are more than 1 solution for $y = \phi x$, let them be x_1, x_2 be two solutions among them.

Let x_1 contain $(x_1)_a, (x_1)_b$ as the two non zero elements as the signal is 2 sparse. Similarly x_2 contain $(x_2)_c, (x_2)_d$ as the non zero elements.

Now,

$$y = \phi x \implies y = (\phi)_a (x_1)_a + (\phi)_b (x_1)_b, (\phi)_i \text{ represents } i\text{th column vector in } \phi$$

Similarly we can write $y = (\phi)_c (x_2)_c + (\phi)_d (x_2)_d$

From these two equations we can say that

$$y = (\phi)_a (x_1)_a + (\phi)_b (x_1)_b = (\phi)_c (x_2)_c + (\phi)_d (x_2)_d \implies (x_2)_c (\phi)_c + (x_2)_d (\phi)_d - (x_1)_a (\phi)_a - (x_1)_b (\phi)_b = 0$$

but as any four columns in ϕ are linearly independent there doesn't exist a solution satisfying above equation. Therefore, there exists a unique solution satisfying $y = \phi x$. We can estimate x by finding a sparse representation basis like DCT or DFT and use OMP to estimate the signal.

Question 5.

(a) Similarities.

1. Most of the hardware used in CACTI is same as the Hitomi Camera, like Objective Lens , Relay Lens and CCD array to convert the intensity of light into electrical signals.
2. Both the techniques make use of coded snapshots for better reconstruction of the image acquired by the lens, and yielding far superior temporal resolution without sacrificing the spatial resolution.

Differences.

1. The coded aperture used in CACTI is lithographically-patterned chrome-on-quartz where as the one used in the Hitomi Camera is Liquid on Crystal on Silicon (LCoS)
2. CACTI's passive coding scheme facilitates scalability without increasing power usage; one may simply use a larger coded aperture to modulate larger values of N pixels with negligible additional on-board power overhead.
This passive coding scheme holds other advantages, such as compactness and polarization independence, over reflective LCoS-based modulation strategies, whereby the additional bandwidth required to modulate the datacube increases proportionally to N.(N=number of pixels)
3. The Hitomi camera uses KSVD and OMP to reconstruct the images whereas CACTI uses TwIST to solve the unconstrained optimization problem

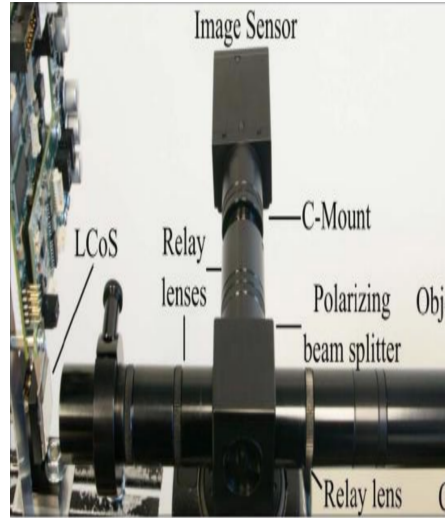


Figure 1: Hitomi et al, ICCV 2011 - Single coded exposure Photographs

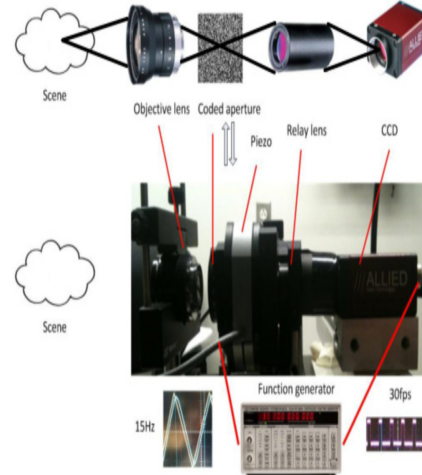


Figure 2: Coded Aperture Compressive Temporal Imaging - CACTI

- (b) The reconstruction algorithm used in CACTI is called TwIST, it works in the following way:-

$$f_e = \operatorname{argmin}_f \|g - Hf\|^2 + \lambda \Omega(f)$$

where $\Omega(f)$ and λ are the regularizer and regularization weights, respectively. This $\Omega(f)$ is the Total Variation (TV) norm given by

$$\Omega(f) = \sum_{i=1}^{N_f} \sum_{i,f}^N \sqrt{(f_{i+1,j,k} - f_{i,j,k})^2 + (f_{i+1,j,k} - f_{i,j,k})^2}$$

Here N= Total number of pixels, N_f = Number of frames, f_e is the N_f -frame estimate of the continuous motion f
 f = Estimated Image data.

Question 6.

- (a) **Title:-** *Compressed Sensing for Fast Electron Microscopy*. **Published year:-2014** **Published at.** Proposed for presentation at the TMS 2014 held February 16-20, 2014 in San Diego, CA.
TMS2014 Annual Meeting Supplemental Proceedings TMS (The Minerals, Metals Materials Society), 2014

Reference:- [here](#).

Keywords:- scanning electron microscope, compressed sensing

- (b) Hardware architecture.

The apparatus used is SEMs which are single-detector instruments that acquire images by raster scanning a focused beam of electrons across the sample, typically in raster-order. At each location, electrons in the incident beam interact with sample, producing various signals about the composition or topography of the sample's surface. These signals may be detected and digitally assigned to the image pixel value at the corresponding sample location. The electron probe is then re positioned via electromagnetic or electrostatic deflection to the subsequent pixel location. Noise in these measurements are mainly due to two factors, back scatter electron (BSE) emissions, which are a result of elastic scattering of incident electrons, and secondary electrons (SE), which are lower-energy electrons that are dislodged from orbitals of specimen atoms through inelastic scattering. BSE images provide sharp contrast at transitions between the atomic number of materials, whereas, since interactions occur within only the first few nanometers of a sample's surface, SE images are primarily topographical in nature. Noise for both **BSE** and **SE** images is multiplicative (Poisson-like), wherein the noise power is proportional to the signal intensity. They make use of a single electron probe positioned at random locations within the field-of-view, so that in theory, ϕ consists of M randomly drawn rows of the identity matrix; ϕ is chosen as a block-DCT basis, which provides good compressibility of smooth electron micrographs, and also results in low mutual coherence for compressed sensing inversion.

- (c) Reconstruction technique + cost function

Reconstructing electron micrographs from measurements $y = \phi x + n$, where n has noise with power σ^2 , was achieved by solving a total-variation regularized version of basis pursuit

$$\min_x \|\Psi^T x\|_1 + \|\nabla x\|_1$$

$$s.t. \|y - \phi x\| \leq \sigma^2$$

The total variation regularizer $\|\nabla x\|_1 = \sum_i \sqrt{|(\nabla_h x)_i|^2 + |(\nabla_v x)_i|^2}$ was included for denoising and to promote smooth boundaries between blocks.

It is Experimentally observed that sufficiently high-quality reconstructions were achieved with 20–50 iterations of our algorithm. The cost function for the following process is $M = O(uK \log N)$.

Few examples for the following process are:-

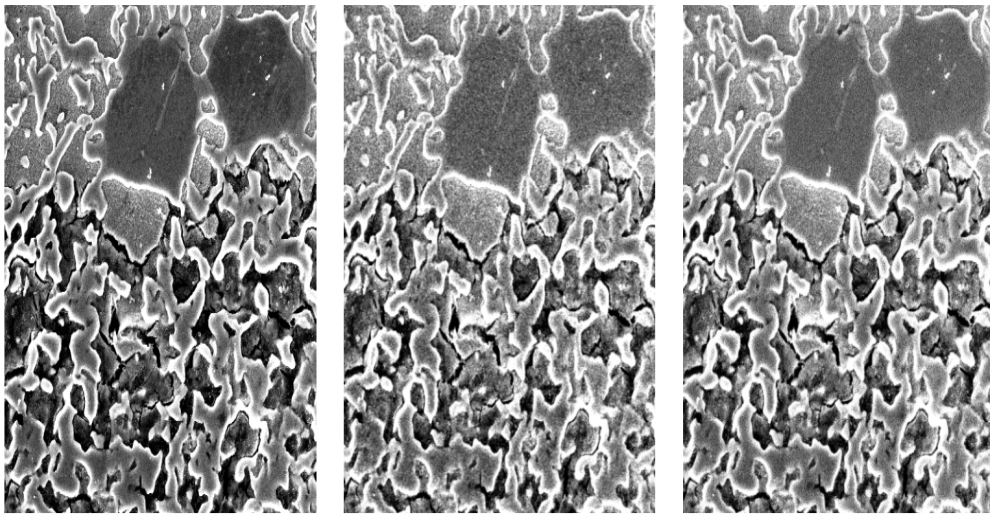


Figure 3: (left) High SNR SEM image of region of interest on the Gibeon sample; (middle) a low-SNR image from a SEM scan; (right) a synthetic image generated from multiple collated SEM image scans.

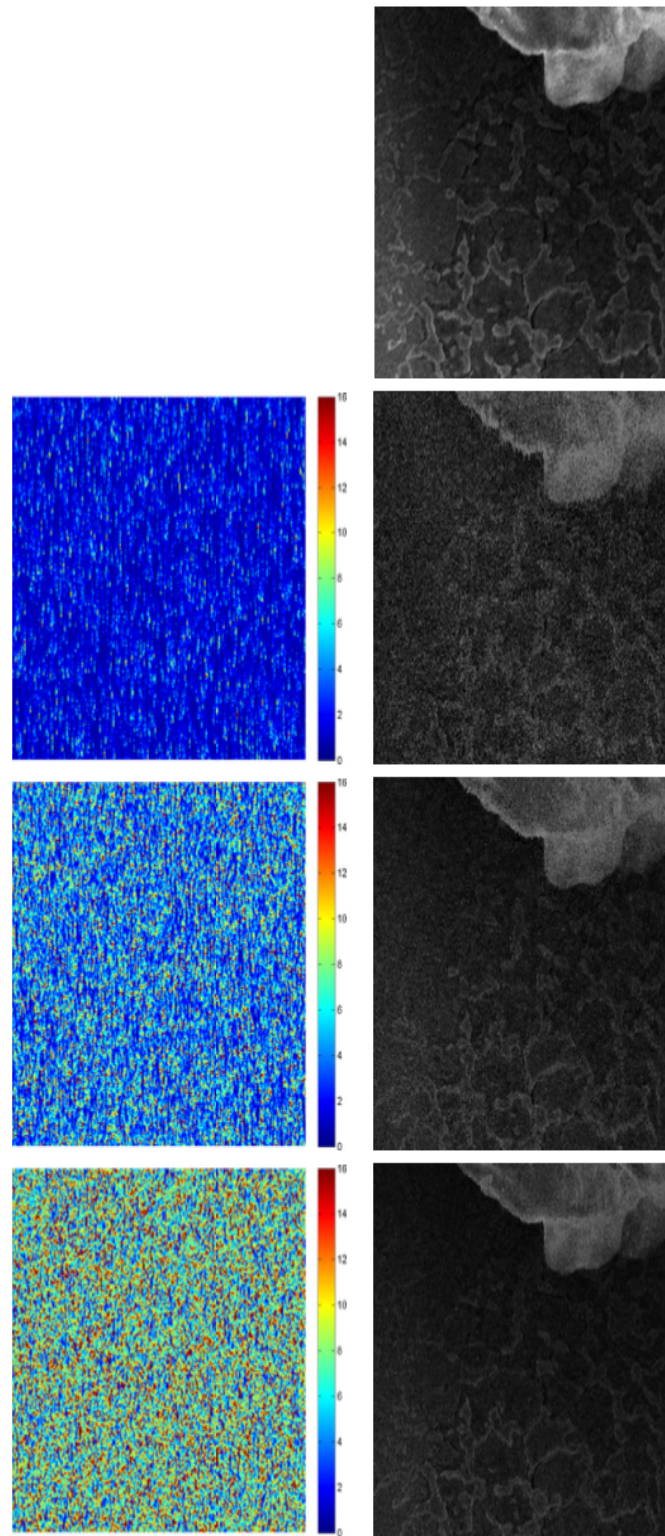


Figure 2: (top) Standard SEM image of the Gibeon sample; (2nd row) 10% sparse, modeled sample locations (left) and reconstruction (right); (3rd row) 30% sparse, modeled sample locations (left) and reconstruction (right); (4th row) 50% sparse, modeled sample locations (left) and reconstruction (right). The colors in the left column represent the number of times the probe visited the given pixel. The electron probe scans in the vertical direction. In addition to sample quality, notice the difference in sample charging.